

ACCELERATED COMPUTATION OF VISCOUS INCOMPRESSIBLE FLOWS WITH HEAT TRANSFER

Seungsoo Lee
Graduate Student

George S. Dulikravich
Associate Professor

Department of Aerospace Engineering
The Pennsylvania State University
University Park, PA 16802, USA

ABSTRACT

A new method for enhancing convergence rate of iterative schemes for the numerical integration of systems of partial differential equations has been developed. It is termed the Distributed Minimal Residual (DMR) method. The DMR method has been applied to incompressible Navier-Stokes equations with heat transfer. All numerical test cases were obtained using explicit four stage Runge-Kutta or Euler implicit time integration. The DMR method was found to reduce the computation time by 20-60% depending on the test case. The formulation for the DMR method is general in nature and can be applied to explicit and implicit iterative algorithms for arbitrary systems of partial differential equations.

INTRODUCTION

A free convection flow is produced by buoyancy forces. Temperature gradients in the fluid are introduced, for example, through boundaries maintained at different temperatures. The resulting fluid density differences induce the motion: hot fluid tends to rise, while cold fluid tends to descent. One of the classical problems of free convection is Benard convection problem (Drazin and Reid, 1981). Two infinite horizontal plates are maintained at different uniform temperatures. The temperature of the bottom wall is higher than that of the upper wall. The basic solution to the problem is no flow with light fluid below heavy fluid. However, when non-dimensional parameter known as Rayleigh number, $Ra = \frac{g\alpha L^3 \Delta T_c}{\kappa \nu}$ exceeds a certain critical value, that is, when the temperature difference is so large that the density difference overcomes the stabilizing effect of viscosity and thermal conductivity, an instability occurs, resulting in fluid motion. Here, g is the gravitational acceleration, α is the coefficient of thermal expansion, $\Delta T_c = T_0 - T_c$ is the characteristic temperature difference, L is the characteristic length (in our example, the distance between the two plates), and κ and ν are the thermal diffusivity and the kinematic viscosity of the fluid, respectively.

Numerical studies of the free convection problems are challenging. The strong source terms of buoyancy forces usually cause numerical instability and often make numerical schemes fail to converge. In this paper,

formulation of two-dimensional heat-conducting viscous flow under the action of buoyancy force will be described. Effectiveness of the DMR method (Dulikravich et al., 1988; Lee et al., 1988, 1989 a,b,c; Lee, 1990) in the presence of strong source terms will be examined.

INCOMPRESSIBLE NAVIER-STOKES EQUATIONS WITH HEAT TRANSFER

The governing equations of motion for a heat-conducting viscous fluid under the action of gravity can be written with the aid of Boussinesq approximation (Tritton, 1977 and Drazin and Reid, 1981) resulting in

$$\frac{\partial Q}{\partial t} + \frac{\partial E}{\partial x} + \frac{\partial F}{\partial y} = S \left\{ \frac{\partial^2 Q}{\partial x^2} + \frac{\partial^2 Q}{\partial y^2} \right\} + H \quad (1)$$

Here, the generalized vectors for non-dimensional variables are

$$Q = \begin{bmatrix} 0 \\ u \\ v \\ \theta \end{bmatrix} \quad E = \begin{bmatrix} u \\ u^2 + p \\ uv \\ u\theta \end{bmatrix} \quad F = \begin{bmatrix} v \\ vu \\ v^2 + p \\ v\theta \end{bmatrix} \\ S = \frac{1}{Gr^{1/2}} \begin{bmatrix} 0 \\ 1 \\ 1 \\ \frac{1}{Pr} \end{bmatrix} \quad H = \begin{bmatrix} 0 \\ n_x \theta \\ n_y \theta \\ 0 \end{bmatrix} \quad (2)$$

where u, v are the velocity vector components, p is the sum of hydrostatic pressure and hydrodynamic pressure, $\theta = \frac{T - T_c}{\Delta T_c}$ is the non-dimensional temperature, and the vector $\hat{n} = \hat{e}_x n_x + \hat{e}_y n_y$ is the upward unit vector assuming that the gravitational force is acting downward. Here, Pr is the Prandtl number, $\frac{\nu}{\kappa}$, Gr is the Grashof number, $\frac{g\alpha L^3 \Delta T_c}{\nu^2}$. Notice that Boussinesq approximation neglects viscous dissipation in the energy equations. Equations (1) must be

considered simultaneously, not like incompressible Navier-Stokes equations which are decoupled from the energy equation when $v \neq v(T)$.

To solve the system of equations, the solution vector Q was modified by adding the artificial compressibility term $\frac{\partial(p/\beta)}{\partial t}$ where β is the artificial compressibility coefficient (Chorin, 1967; Kwak et al., 1986).

For the completeness, let us consider the mixed convection problem. The solution vector and the flux vectors for the mixed convection problem remain the same as for the natural convection problem. Only changes in the Eq. (2) are (White, 1974)

$$S = \frac{1}{Re} \begin{bmatrix} 0 \\ 1 \\ 1 \\ \frac{1}{Pr} \end{bmatrix} \quad H = \frac{Gr}{Re^2} \begin{bmatrix} 0 \\ n_x \theta \\ n_y \theta \\ 0 \end{bmatrix} \quad (3)$$

The equation (1) is transformed to a general curvilinear ξ, η non-orthogonal coordinate system

$$\frac{\partial \tilde{Q}}{\partial t} + \frac{\partial \tilde{E}}{\partial \xi} + \frac{\partial \tilde{F}}{\partial \eta} = D^2(J\tilde{Q}) + \tilde{H} \quad (4)$$

where

$$\tilde{Q} = \frac{1}{J} \begin{bmatrix} p \\ \beta \\ u \\ v \\ \theta \end{bmatrix} \quad \tilde{E} = \frac{1}{J} \begin{bmatrix} U \\ Uu + \xi_x p \\ Uv + \xi_y p \\ U\theta \end{bmatrix} \quad \tilde{F} = \frac{1}{J} \begin{bmatrix} V \\ Vu + \eta_x p \\ Vv + \eta_y p \\ V\theta \end{bmatrix} \quad (5)$$

$$\tilde{H} = \frac{1}{J} \begin{bmatrix} 0 \\ n_x \theta \\ n_y \theta \\ 0 \end{bmatrix}$$

For a mixed convection problem, the source vector is modified to

$$\tilde{H} = \frac{Gr}{JRe^2} \begin{bmatrix} 0 \\ n_x \theta \\ n_y \theta \\ 0 \end{bmatrix} \quad (6)$$

Here, J is the Jacobian determinant, while U and V are the contravariant velocity vector components normal to constant ξ and η grid line, respectively.

The physical viscous terms are contained in

$$D^2(J\tilde{Q}) = \left[\frac{S}{J} g_{ij} (J\tilde{Q})_{,j} \right]_{,i} \quad (7)$$

where g_{ij} is the contravariant metric tensor, $g_{ij} = \nabla x'_i \nabla x'_j$.

EIGENVALUE ANALYSIS

The Jacobians of the inviscid part of the modified Navier-Stokes equations in Cartesian coordinates are given as

$$A = \frac{\partial E}{\partial Q} = \begin{bmatrix} 0 & 1 & 0 & 0 \\ \beta & 2u & 0 & 0 \\ 0 & v & u & 0 \\ 0 & \theta & 0 & u \end{bmatrix} \quad B = \frac{\partial F}{\partial Q} = \begin{bmatrix} 0 & 0 & 1 & 0 \\ 0 & v & u & 0 \\ \beta & 0 & 2v & 0 \\ 0 & 0 & \theta & v \end{bmatrix} \quad (8)$$

The Jacobians in the generalized curvilinear coordinates are easily obtained from those defined in Cartesian coordinates. Thus,

$$\tilde{A} = \frac{\partial \tilde{E}}{\partial \tilde{Q}} = K(U, \xi_x, \xi_y) \quad \tilde{B} = \frac{\partial \tilde{F}}{\partial \tilde{Q}} = K(V, \eta_x, \eta_y) \quad (9)$$

where

$$K(k, k_1, k_2) = k_1 \frac{\partial E}{\partial Q} + k_2 \frac{\partial F}{\partial Q}$$

$$= \begin{bmatrix} 0 & k_1 & k_2 & 0 \\ \beta k_1 & k+k_1 u & k_2 u & 0 \\ \beta k_2 & k_1 v & k+k_2 v & 0 \\ 0 & k_1 \theta & k_2 \theta & k \end{bmatrix} \quad (10)$$

where k_1 and k_2 can be either ξ_x and ξ_y or η_x and η_y depending on the direction to be considered. Also, k is defined as

$$k = k_1 u + k_2 v \quad (11)$$

The eigenvalues of the matrix K are given by

$$\Lambda = \text{diag}(k - c, k + c, k, k) \quad (12)$$

where the equivalent speed of sound, c , is given as

$$c = \sqrt{k^2 + \beta(k_1^2 + k_2^2)} \quad (13)$$

NUMERICAL ALGORITHMS

In this section, the numerical algorithms used for incompressible Navier-Stokes equations with energy equation will be discussed. Two time integration schemes (explicit four stage Runge-Kutta time stepping method, and

Euler implicit method) were used in conjunction with the central difference spatial discretization scheme.

The fourth order artificial dissipation of Steger and Kutler (1977)

$$D(J\tilde{Q}) = \frac{\epsilon}{8J\Delta t} \nabla^4 [J\tilde{Q}] \quad (14)$$

was added to the residual vector R , resulting in the complete residual.

$$\hat{R} = \frac{\partial \tilde{E}}{\partial \xi} + \frac{\partial \tilde{F}}{\partial \eta} - D^2(J\tilde{Q}) - \tilde{H} + D(J\tilde{Q}) \quad (15)$$

The Runge-Kutta time stepping method (Jameson, 1981) can be written as

$$\begin{aligned} \tilde{Q}^0 &= \tilde{Q}^t \\ \Delta \tilde{Q}^k &= -\alpha_k \Delta t \hat{R}^{k-1} \quad k = 1, 2, \dots, K \\ \tilde{Q}^{t+1} &= \tilde{Q}^t + \Delta \tilde{Q}^K \end{aligned} \quad (16)$$

where α_k are the coefficients for each of the K stages of the Runge-Kutta scheme required to advance the solution from the iteration level t to the iteration level $t+1$. For example, $\alpha_k = 1/4, 1/3, 1/2$ and 1 for the four stage Runge-Kutta scheme. To reduce the computational effort, the artificial dissipation and the viscous part of the residual are calculated only at the beginning of the first stage of each application of the Runge-Kutta scheme, and kept unchanged during the four stages of the Runge-Kutta scheme.

The Euler implicit scheme for incompressible Navier-Stokes equations with energy equation is

$$\tilde{Q}^{t+1} = \tilde{Q}^t + \Delta t \frac{\partial}{\partial t} \tilde{Q}^{t+1} + O(\Delta t^2) \quad (17)$$

or

$$\Delta \tilde{Q} = -\Delta t \left[\frac{\partial \tilde{E}}{\partial \xi} + \frac{\partial \tilde{F}}{\partial \eta} - D^2(J\tilde{Q}) - \tilde{H} \right]^{t+1} \quad (18)$$

where $\Delta \tilde{Q} = \tilde{Q}^{t+1} - \tilde{Q}^t$. The flux vectors and source terms are linearized by expanding in Taylor series, and truncating terms higher than second order in time, that is,

$$\begin{aligned} \tilde{E}^{t+1} &= \tilde{E}^t + \tilde{A} \Delta \tilde{Q} \\ \tilde{F}^{t+1} &= \tilde{F}^t + \tilde{B} \Delta \tilde{Q} \\ \tilde{H}^{t+1} &= \tilde{H}^t + \tilde{D} \Delta \tilde{Q} \end{aligned} \quad (19)$$

where

$$\tilde{D} = \frac{\partial \tilde{H}}{\partial \tilde{Q}} = \begin{bmatrix} 0 & 0 & 0 & 0 \\ 0 & 0 & 0 & n_x \\ 0 & 0 & 0 & n_y \\ 0 & 0 & 0 & 0 \end{bmatrix} \quad (20)$$

The mixed second order derivatives, however, are treated explicitly in order to use the factorization technique. The Eq. (18) then becomes

$$\begin{aligned} \Delta \tilde{Q} &= \\ -\Delta t \left\{ \frac{\partial}{\partial \xi} \tilde{A} + \frac{\partial}{\partial \eta} \tilde{B} - \frac{\partial}{\partial \xi} \left(\frac{S_{g11}}{J} \frac{\partial}{\partial \xi} \right) - \frac{\partial}{\partial \eta} \left(\frac{S_{g22}}{J} \frac{\partial}{\partial \eta} \right) - \tilde{D} \right\} \Delta \tilde{Q} \\ - \Delta t \left[\frac{\partial \tilde{E}}{\partial \xi} + \frac{\partial \tilde{F}}{\partial \eta} - D^2(J\tilde{Q}) - \tilde{H} \right]^t \end{aligned} \quad (21)$$

By applying the factorization scheme and adding the artificial dissipation to the right hand side, we have

$$\begin{aligned} \left[P + \Delta t \left\{ \frac{\partial}{\partial \xi} \tilde{A} - \frac{\partial}{\partial \xi} \left(\frac{S_{g11}}{J} \frac{\partial}{\partial \xi} \right) \right\} \right] P^{-1} \\ \left[P + \Delta t \left\{ \frac{\partial}{\partial \eta} \tilde{B} - \frac{\partial}{\partial \eta} \left(\frac{S_{g22}}{J} \frac{\partial}{\partial \eta} \right) \right\} \right] \Delta \tilde{Q} = -\Delta t \hat{R}^t \end{aligned} \quad (22)$$

where $P = I - \Delta t \tilde{D}$.

BOUNDARY CONDITIONS

At the solid wall, the normal momentum equation is used, instead of zero order boundary layer approximation, $\frac{\partial p}{\partial n} = 0$. It can easily be shown that in the presence of buoyancy force, the boundary layer approximation gives erroneous results since the momentum equations contain the buoyancy terms. The normal momentum equation for $\xi = \text{constant}$ line is found to be

$$\frac{\partial}{\partial \xi} [\beta J \tilde{q}_1] = \eta_y [D^2(J\tilde{q}_2) + \tilde{h}_2] - \eta_x [D^2(J\tilde{q}_3) + \tilde{h}_3] \quad (23)$$

where \tilde{q} are the terms of \tilde{Q} and \tilde{h} are the terms of \tilde{H} .

Now, we discuss the implementation of Eq. (23). For the explicit scheme, $(\beta J \tilde{q}_1)_\xi$ is computed at the first grid point off the wall. Then, \tilde{q}_1 at the vertical wall is extrapolated from $(\beta J \tilde{q}_1)_\xi$ and the value of \tilde{q}_1 one grid point off the wall. Non-slip boundary conditions ($u = v = 0$) are imposed at the wall. The wall temperature is set to a given value for the thermal Dirichlet boundary condition, while the temperature is extrapolated from the interior point for the thermal Neumann boundary condition.

For the Euler implicit method, Eq. (23) is written in delta form as

$$\begin{aligned} \frac{\partial}{\partial \xi} [\beta J \Delta \tilde{q}_1] = \\ - \frac{\partial}{\partial \xi} [\beta J \tilde{q}_1] + \eta_y [D^2(J\tilde{q}_2) + \tilde{h}_2] - \eta_x [D^2(J\tilde{q}_3) + \tilde{h}_3] \end{aligned} \quad (24)$$

If the wall is insulated, then the boundary condition vector is $\tilde{\Omega} = (0, u, v, \theta_w - \theta_i)^T$, where the subscripts, w and i denote grid indices at the wall and at the first grid layer off the wall, respectively. Then

$$\frac{\partial \tilde{\Omega}}{\partial \tilde{Q}_w} \Delta \tilde{Q}_w - \frac{\partial \tilde{\Omega}}{\partial \tilde{Q}_i} \Delta \tilde{Q}_i = 0 \quad (25)$$

Upon adding Eq. (24) and Eq. (25), it follows that $\hat{A} \Delta \tilde{Q}_w - \hat{B} \Delta \tilde{Q}_i = \hat{C}$, where $\hat{A} = \text{diag}(\beta J_w, J_w, J_w, J_w)$, and $\hat{B} = \text{diag}(\beta J_i, 0, 0, J_i)$, and

$$\hat{C} = \begin{bmatrix} \text{R.H.S. of Eq. (24)} \\ 0 \\ 0 \\ 0 \end{bmatrix} \quad (26)$$

For a mixed convection problem, we encounter inflow and exit boundaries. The boundary treatment utilizes the characteristic boundary condition treatment (Chakravarthy, 1982). At the inflow boundary, we have three positive eigenvalues and one negative eigenvalue. Thus, u and v components of the velocity vector were specified with the temperature profile. At the exit, three positive eigenvalues and one negative eigenvalue indicate that one boundary condition (back pressure) was imposed.

DISTRIBUTED MINIMAL RESIDUAL METHOD

The local residual at iteration level $t+1$ is given by

$$\hat{R}^{t+1} = \frac{\partial \tilde{E}^{t+1}}{\partial \xi} + \frac{\partial \tilde{F}^{t+1}}{\partial \eta} - D^2(J\tilde{Q}^{t+1}) - \tilde{H}(\tilde{Q}^{t+1}) + D(J\tilde{Q}^{t+1}) \quad (27)$$

Assume that the solution at iteration level $t+1$ is extrapolated from the previous M consecutive iteration levels. Then, one can say that

$$\tilde{Q}^{t+1} = \tilde{Q}^t + \sum_{m=1}^M \Theta^m \quad (28)$$

where

$$\Theta^m = \begin{bmatrix} \omega_1^m \Delta_1^m \\ \omega_2^m \Delta_2^m \\ \omega_3^m \Delta_3^m \\ \omega_4^m \Delta_4^m \end{bmatrix} \quad (29)$$

Here, ω 's are the acceleration factors to be calculated, Δ 's are the corrections computed with the original scheme, M denotes the total number of consecutive iteration steps combined.

Using Taylor series expansion in time and truncating the terms that are higher than second order in Δt , Eq. (27) becomes approximately

$$\hat{R}^{t+1} = \hat{R}^t + \sum_{m=1}^M \left[\frac{\partial}{\partial \xi} \tilde{A}^t + \frac{\partial}{\partial \eta} \tilde{B}^t - D^2 J - \tilde{D} + D J \right] \Theta^m \quad (30)$$

The global domain residual can be defined as

$$\hat{R}^t = \sum_D \hat{R}^{tT} \hat{R}^t \quad (31)$$

In order to minimize the \hat{R}^{t+1} , the ω 's are chosen from the following equations

$$\frac{\partial \hat{R}^{t+1}}{\partial \omega_r^m} = 0 \quad (32)$$

that is,

$$\begin{aligned} & - \sum_D \hat{R}^{tT} \left[\frac{\partial}{\partial \xi} \tilde{A}^t + \frac{\partial}{\partial \eta} \tilde{B}^t - D^2 J - \tilde{D} + D J \right] \frac{\partial \Theta^m}{\partial \omega_r^m} \\ & = \sum_D \sum_n \left\{ \left[\frac{\partial}{\partial \xi} \tilde{A}^t + \frac{\partial}{\partial \eta} \tilde{B}^t - D^2 J - \tilde{D} + D J \right] \Theta^n \right\}^T \\ & \quad \left\{ \left[\frac{\partial}{\partial \xi} \tilde{A}^t + \frac{\partial}{\partial \eta} \tilde{B}^t - D^2 J - \tilde{D} + D J \right] \frac{\partial \Theta^m}{\partial \omega_r^m} \right\} \quad (33) \end{aligned}$$

where

$$\frac{\partial \Theta^m}{\partial \omega_r^m} = \left[\Delta_p^m \delta_{pr} \right] \quad (34)$$

δ_{pr} is the Kronecker delta and transcript T denotes transpose of a matrix. Notice the following identity,

$$\Theta^n = \sum_q \omega_q^n \frac{\partial \Theta^n}{\partial \omega_q^n} \quad (35)$$

Also, notice $\frac{\partial \Theta^n}{\partial \omega_q^n}$ is not a function of ω .

Let

$$\mathbf{a}_q^m = \left[\frac{\partial}{\partial \xi} \tilde{A}^t + \frac{\partial}{\partial \eta} \tilde{B}^t - D^2 J - \tilde{D} + D J \right] \frac{\partial \Theta^m}{\partial \omega_q^m} \quad (36)$$

Then Eq. (33) becomes

$$- \sum_D \hat{R}^{tT} \mathbf{a}_r^m = \sum_n \sum_q \sum_D \omega_q^n \mathbf{a}_q^{nT} \mathbf{a}_r^m \quad (37)$$

For simplicity, let

$$\mathbf{c}_{qr}^{nm} = \sum_D \mathbf{a}_q^{nT} \mathbf{a}_r^m \quad \mathbf{b}_r^m = - \sum_D \hat{R}^{tT} \mathbf{a}_r^m \quad (38)$$

so that Eq. (37) can be written as

$$\sum_n^M \sum_q^4 \omega_q^n c_{qr}^{nm} = b_r^m \quad (39)$$

representing the system of $4 \times M$ linear algebraic equations for the $4 \times M$ optimum acceleration factors ω . For example, if we are to combine $M = 2$ consecutive iteration steps to extrapolate the solution, we periodically need to solve 8 equations for 8 values of ω .

COMPUTATIONAL RESULTS

It is known that for the case of a natural convection between two infinite parallel plates the critical Rayleigh number is approximately $Ra = 1708$ (Drazin and Reid, 1981). When the Rayleigh number is larger than the critical value, a fluid motion occurs which is driven by the buoyancy force. Due to the difficulty associated with numerically simulating infinite parallel plates, a finite computational domain surrounded by solid walls was considered in this study. The aspect ratio of the computational domain was chosen to be 3. The bottom wall is uniformly heated, while the upper wall is uniformly cooled. Both side walls are thermally insulated. The wall boundary condition on pressure was obtained from the normal momentum equation. A mildly clustered grid of 60×30 cells was used (Fig. 1). Two different cases were computed with both the Runge-Kutta (RK) time stepping method and the Euler implicit method.

First, the flow with the Grashof number $Gr = 3000$ and the Prandtl number $Pr = 1$ (that is $Ra = 3000$) was computed. CFL = 2.8 and von Neumann number $\sigma = 0.4$ were used in this computation for the RK method, while CFL = 10 was used for the Euler implicit method. The artificial compressibility coefficient β providing the fastest convergence was found to be $\beta = 5$ for the RK method, while it was $\beta = 1$ for the Euler implicit method. No artificial dissipation has been added for these computations. The convergence histories (Fig. 2) show that the DMR accelerated the basic RK method, resulting in 20 % reduction in CPU time. Figure 3 shows that the computational savings in terms of both number of iterations and the CPU time were achieved by using the DMR method with the Euler implicit method. Figure 4 presents the computed solutions, which agrees very well with the solution from the RK method. It is noticeable that the isobar contours are not normal to the wall, which implies that the boundary condition of $\frac{\partial p}{\partial n} = 0$ would have given erroneous results.

In another example, the computational domain was tilted by 30° . The Grashof number in this test case was $Gr = 3000$. The Prandtl number was $Pr = 1$, which corresponds to $Ra = 3000$. The same computational grid was used as in the previous test case. The maximum allowable CFL number of 2.8 and the von Neumann number $\sigma = 0.4$ were used for the RK method, while CFL = 10 was used for the Euler implicit method. Every 30 iterations the DMR method was applied with 2 solutions combined for the RK method. On the other hand, the

DMR method was applied every 10 iterations while combining 2 solutions in the Euler implicit method. The DMR method was able to accelerate both basic schemes (the explicit RK method and the Euler implicit method). The reduction in CPU time was 40 % for the RK method (Fig. 5), and 50 % for the Euler implicit method (Fig. 6). As a result of the tilt in gravitational direction, only one circulatory motion was generated (Fig. 7) with practically identical results obtained when using the RK method.

Finally, one example of mixed convection problem was considered where cool fluid enters a U-shaped channel whose top and bottom walls were heated with the constant temperature. The computational grid of 129×30 cell was used (Fig. 8). Only explicit RK method was used for this test case along with the DMR method. CFL number of 2.8 and von Neumann number of 0.4 were employed in this computation with a fourth order artificial dissipation ($\epsilon = 0.25$). The Grashof number of 3000 was imposed, which denotes the temperature difference between the fluid and the wall. Note that the buoyancy effects for this case are negligible. Effectively, the energy equation is decoupled from the continuity and the momentum equations. Nevertheless, all the equations including energy equation were solved simultaneously in this example. The artificial compressibility coefficient was $\beta = 10$. Figure 9 presents the convergence histories in terms of the number of iterations and the CPU time. With the RK method, reduction of five orders of magnitude in initial residual was achieved in 6000 iterations, while 10 orders of magnitude reduction was achieved with the same number of iterations when the DMR was applied, resulting in 60 % savings in CPU time. The isobar contours and the velocity vector plot (Fig. 10) indicate that a large separation occurs in the curved duct. Isotherm contours show thermal boundary layer on both walls of the channel.

REFERENCES

- Chakravarthy, S. R., "Euler Equations - Implicit Schemes and Implicit Boundary Conditions," AIAA paper 82-0228, AIAA 20th Aerospace Sciences Meeting, Orlando, Florida, Jan. 11-14, 1982.
- Chorin, A. J., "A Numerical Method for Solving Incompressible Viscous Flow Problems," *Journal of Computational Physics*, Vol. 2, 1967, pp. 12-26.
- Drazin, P. and Reid, W., *Hydrodynamic Stability*, Cambridge Monographs on Mechanics and Applied Mathematics, edited by Batchelor, G. K. and Miles, J. W., Cambridge University Press, 1981.
- Dulikravich, G. S., Dorney, D. J. and Lee, S., "Iterative Acceleration and Physically Based Dissipation for Euler Equations of Gasdynamics," *Proceedings of ASME WAM'88*, Symposia on Advances and Applications in Computational Fluid Dynamics, edited by O. Baysal, FED - Vol. 66, 1988, pp. 81-92.
- Jameson, A., Schmidt, W., and Turkel, E., "Numerical Solutions of the Euler Equations by Finite Volume Methods Using Runge-Kutta Time-Stepping Scheme," AIAA paper 81-1259, Palo Alto, CA, June, 1981.
- Kwak, D., Chang, J. L. C., Shanks, S. P. and Chakravarthy, S. R., "An Incompressible Navier-Stokes Flow Solver in Three Dimensional Curvilinear Coordinate System Using Primitive Variables," *AIAA Journal*, Vol. 24, No. 3, March

- 1986, pp. 390-396.
- Lee, S., Dulikravich, G. S. and Dorney, D., "Distributed Minimal Residual (DMR) Method for Explicit Algorithms Applied to Nonlinear Systems," presented at the Conference on Iterative Method for Large Linear Systems, Austin, Texas, Oct. 19-21, 1988.
- Lee, S. and Dulikravich, G. S., "Acceleration of Iterative Algorithms for Euler Equations of Gasdynamics," AIAA Paper 89-0097, Reno, NV, Jan. 1989 a; Also, accepted for publication in AIAA Journal.
- Lee, S. and Dulikravich, G. S., "Accelerated Computation of Viscous, Steady Incompressible Flows," ASME paper 89-GT-45, Gas Turbine and Aeroengine Congress and Exposition, Toronto, Canada, June 4-8, 1989 b.
- Lee, S. and Dulikravich, G. S., "A Fast Iterative Algorithm for Incompressible Navier-Stokes Equations," Proceedings the 10th Brazilian Congress of Mechanical Engineering, Rio de Janeiro, Dec. 7-10, 1989 c.
- Lee, S., Acceleration of Iterative Algorithms for Euler and Navier-Stokes Equations, Ph. D. Thesis, The Department of Aerospace Engineering, The Pennsylvania State University, May 1990.
- Steger, J. L. and Kutler, P., "Implicit Finite-Difference Procedure for the Computation of Vortex Wakes," AIAA Journal, Vol. 15, No. 7, July 1977, pp. 581-590.
- Tritton, D. J., Physical Fluid Dynamics, Van Nostrand Reinhold Company, New York, New York, 1977.
- White, F. W., Viscous Fluid Flow, McGraw-Hill Book Company, New York, New York, 1974.

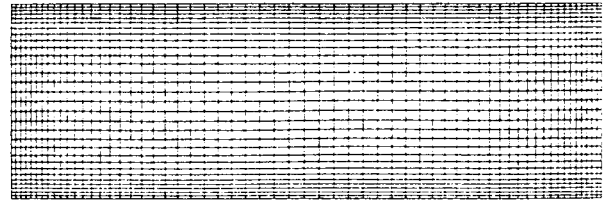
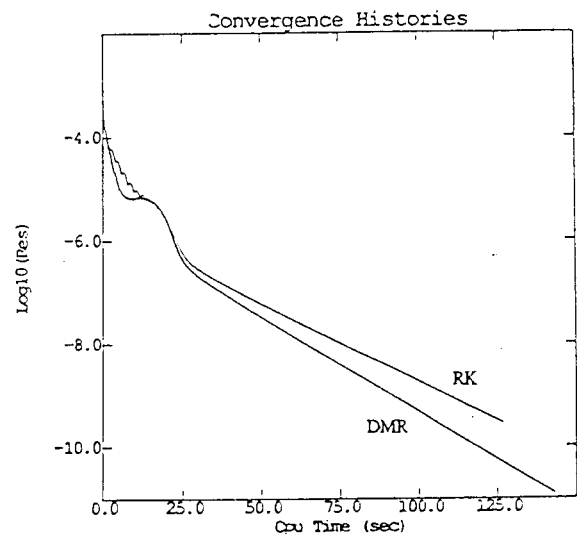
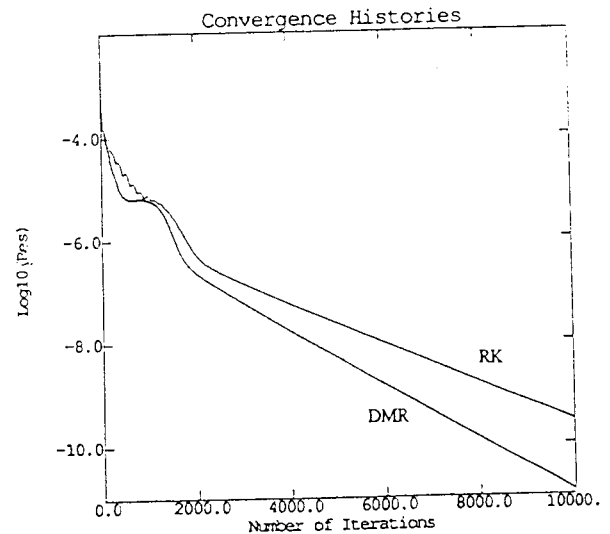


Figure 1 An H-type computational grid of 60x30 cells used for Benard convection problem



problem with Gr = 3000 (RK)

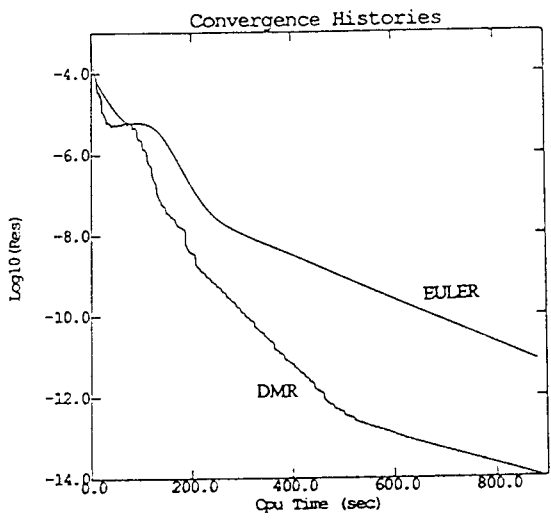
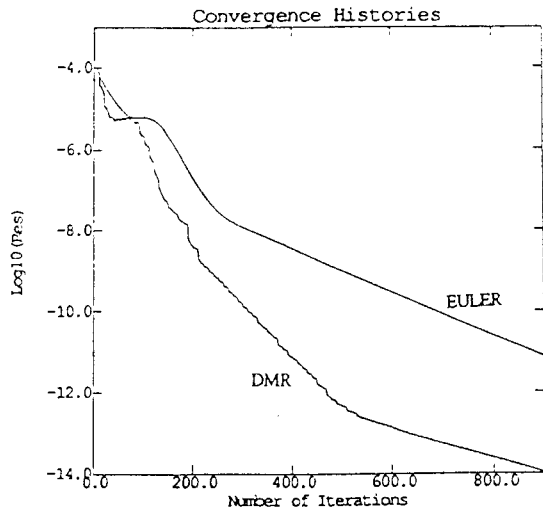
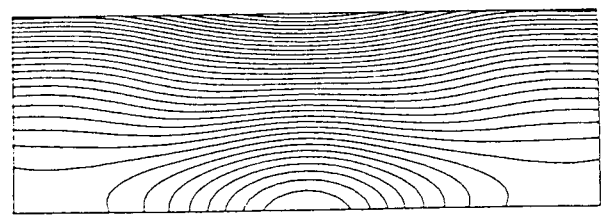
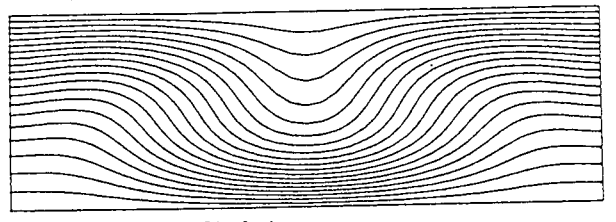


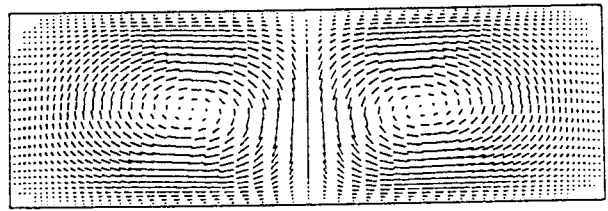
Figure 3 Convergence histories for Benard convection problem with $Gr = 3000$ (Euler implicit)



(a) Isobar contours



(b) Isotherm contours



(c) Velocity vectors

Figure 4 Isobar contours, isotherm contours and velocity vectors for $Gr = 3000$ (Euler Implicit)

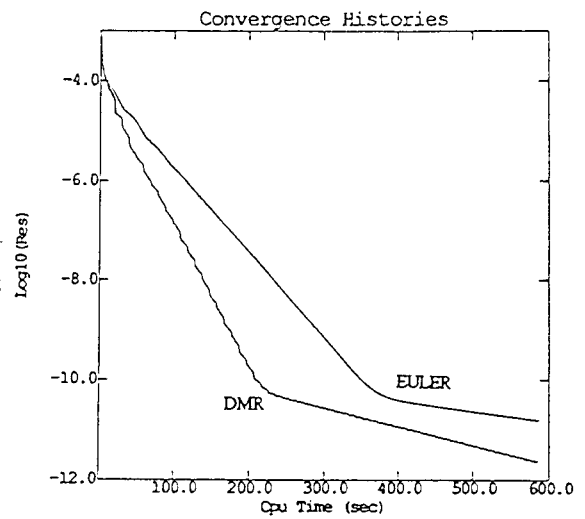
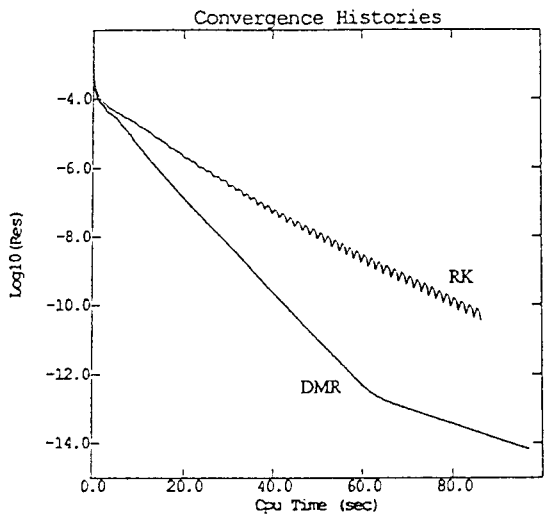
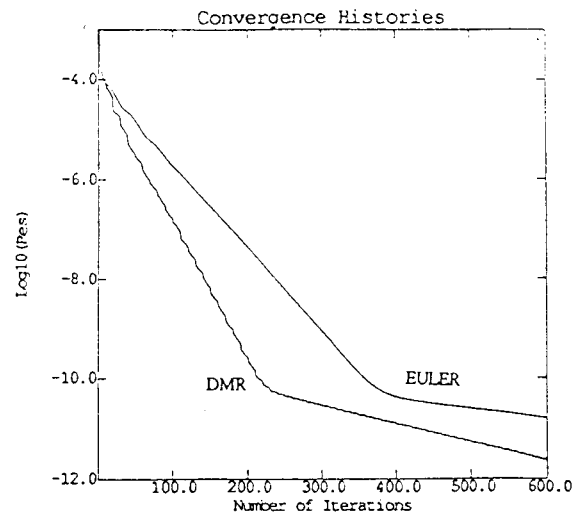
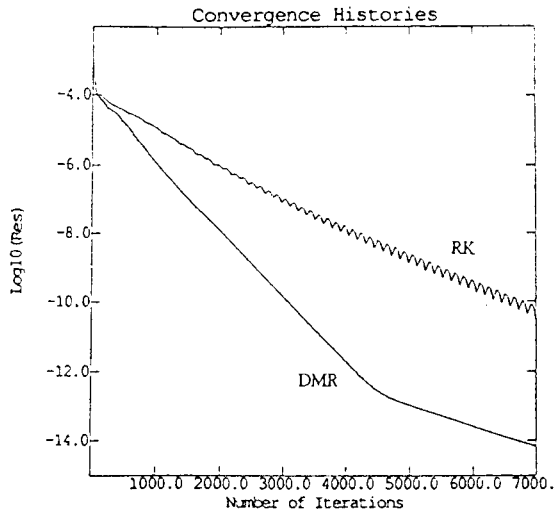


Figure 5 Convergence histories for Benard convection problem with $Gr = 3000$ and $\varphi = 30^\circ$ (RK)

Figure 6 Convergence histories for Benard convection problem with $Gr = 3000$ and $\varphi = 30^\circ$ (Euler implicit)

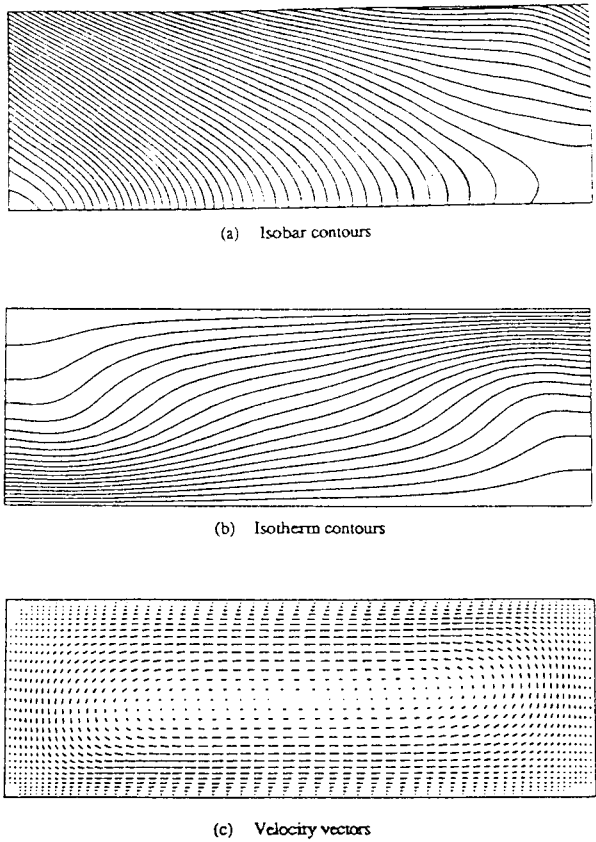


Figure 7 Isotherm contours, isotherm contours and velocity vectors for $Gr = 3000$ and $\phi = 30^\circ$ (Euler Implicit)

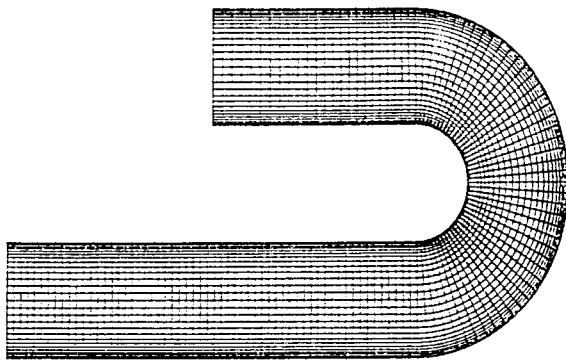


Figure 8 An H-type computational grid of 129×30 cells used for the flow inside U-shaped channel ($Gr = 3000$)

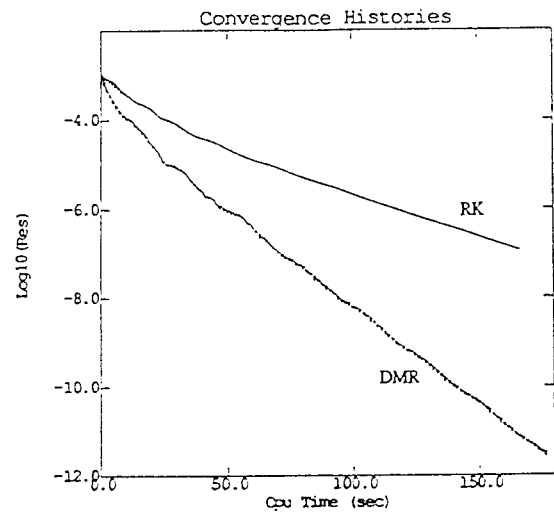
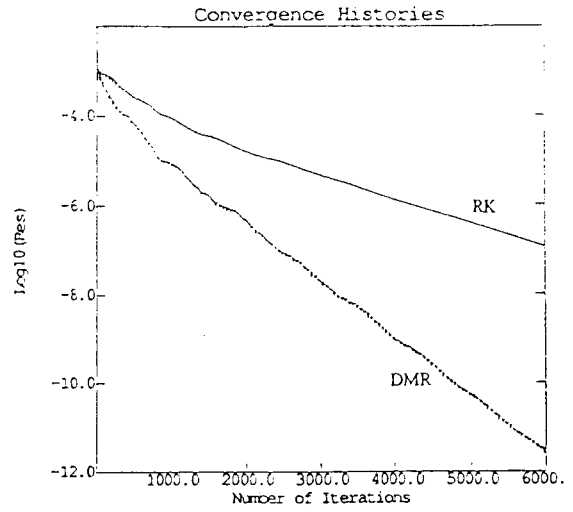
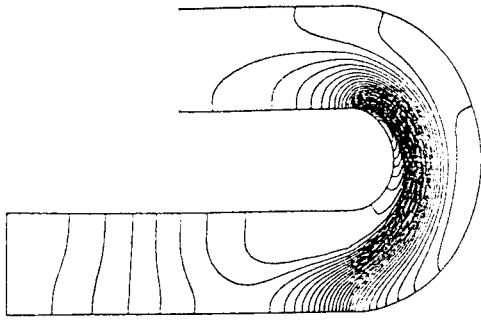
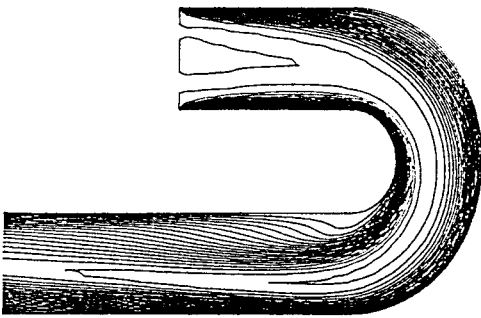


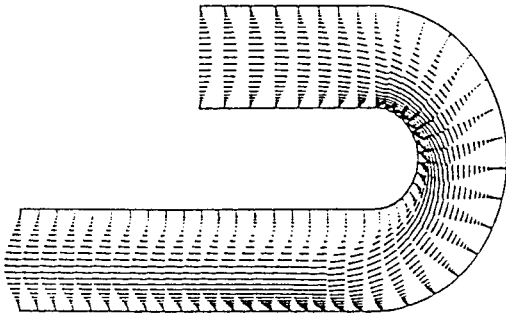
Figure 9 Convergence histories for the flow inside U-shaped channel



(a) Isobar contours



(b) Isotherm contours



(c) Velocity vectors

Figure 10 Isobar, isotherm contours and velocity vectors for the U-shaped channel